XXIst Moriond Astrophysics Meeting - Les Arcs March 10-17, 2001

XMM-Newton observation of M87

Kyoko Matsushita

Max-Planck-Institut für Extraterrestrial Physik, D-85748 Garching, Germany

We report the results of detailed analysis of the temperature structure of the X-ray emitting plasma halo of M 87, the cD galaxy of the Virgo Cluster. The temperature of the intracluster plasma is 0.8 keV at the center and gradually increase to 2.5 keV at 80 kpc. The data provide strong indications that the intracluster medium has a single phase structure locally. The deprojected spectrum at each radius is well fitted by a single temperature MEKAL model, except for the very central region ($<$ 1 arcmin) which seems to be affected by the jet and radio lobe structure. The single-phase nature of the intracluster medium is in conflict with the standard cooling flow model which is based on a multiphase temperature structure. In addition the signature of gas cooling below 0.8 keV to zero temperature is not observed as expected for a cooling flow. The central temperature of the intracluster medium agrees well with the potential depth and the velocity dispersion of the cD galaxy. The latter results implies that the central region of the intracluster medium is equivalent to a virialized interstellar medium in M 87.

1 Introduction

In cores of many clusters, X-ray imaging data show a highly peaked surface brightness profile (e.g. Fabian et al. 1981). The radiative cooling time in these region is much less than a Hubble time. Without a heating process, the gas cools to low temperature and results in a "cooling flow" (Fabian 1994 for a review). The mass flow rate, $\dot{M}$, that is deduced in the standard cooling flow model, is approximately proportional to the radius. This implies that matter is deposited throughout the entire cooling flow region. It also implies that the gas in the cooling flow zone is "multi-phase" on scales small enough that the imhomogenities have escaped the observation so far.

M 87 is the cD galaxy of the nearest rich cluster, the Virgo Cluster. It is very luminous in X-rays, and suggested to have a "cooling flow" with $\dot{M}$ of about $10 M \odot \mathrm{yr}^{-1}$ (Stewart et al. 1984). M 87 also host a central AGN. The radio emission is complex and there are strong two lobe structure. An enhancement of the X-ray emission around the lobe was discovered with the EINSTEIN HRI (Feigelson et al. 1987) and ROSAT PSPC (Böhringer et al. 1995) Early works of an XMM observation of M 87 have already published (Böhringer et al. 2001; Belsole et al. 2001). The projected spectrum is fitted with a single temperature model (Böhringer et al. 2001). The abundance drop at central region is interpreted as resonance scattering. The detailed spectra analysis on the jets and radio lobe structure is shown in Belsole et al. (2001). In this paper, we report more detailed temperature structure using deprojecting analysis, and apply a cooling flow model to the spectral analysis.

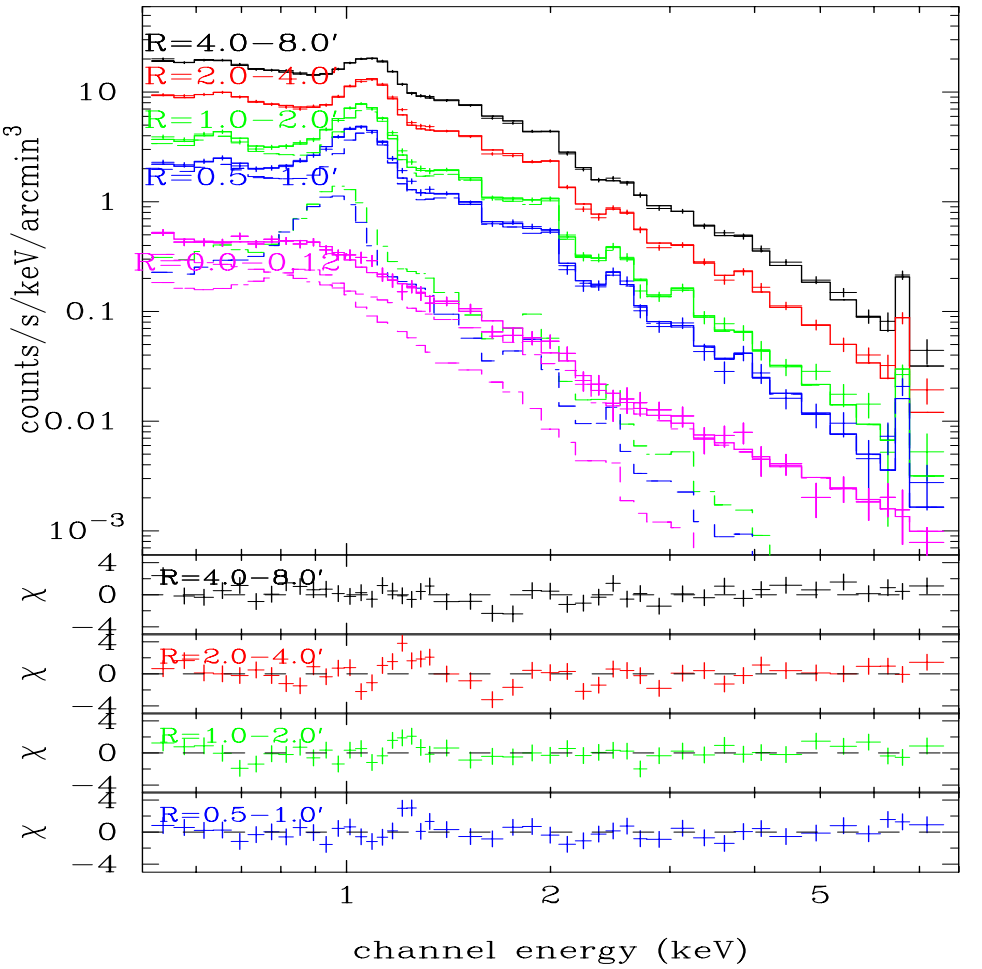

Figure 1: Deprojected spectra of the EPN (lobes excluded). The spectrum of $R < 0.12'$ are fitted with the double component model, consisting a MEKAL model and a power-low component and those of R=0.5-1.0′ and 1.0-2.0′ are fitted with two component MEKAL model. Each component is plotted in dashed lines. The other spectra are fitted with a MEKAL model. Bottom panels show residuals of the fit.

1.1 Observation

M87 was observed with XMM-Newton on June 19th, 2000. The effective exposure of the EPN and the EMOS detector are 30ks and 40 ks for the EPN and the EMOS, respectively, We have excluded regions with excess emission related to the jet and radio lobes and accumulated spectra in annular regions. Deprojected spectra are calculated by subtracting the contribution from outer shell regions assuming the ICM is spherically symmetric as done by Nulsen and Böhringer (1995).

1.2 Temperature structure

The single temperature MEKAL model gives reasonable fits at $R > 2'$. Figure 1 shows the EPN spectra for several deprojected shells, fitted with the MEKAL model. Within $R < 2'$, there are small amount of 1 keV component. The complicated structure within $R < 2'$ in the energy map indicate that the remaining 1 keV component also relate to the activity related to the radio jet and lobes.

At R> 0.5′ the temperature derived from energy range of >1.6 keV ($kT_{\rm hard}$), Si ($kT_{\rm Si}$) and S energy band ($kT_{\rm S}$), of given deprojected spectrum agree within 10%. The temperature obtained from Fe-L band also agrees well with $kT_{\rm hard}$, These result strongly indicate that at least at

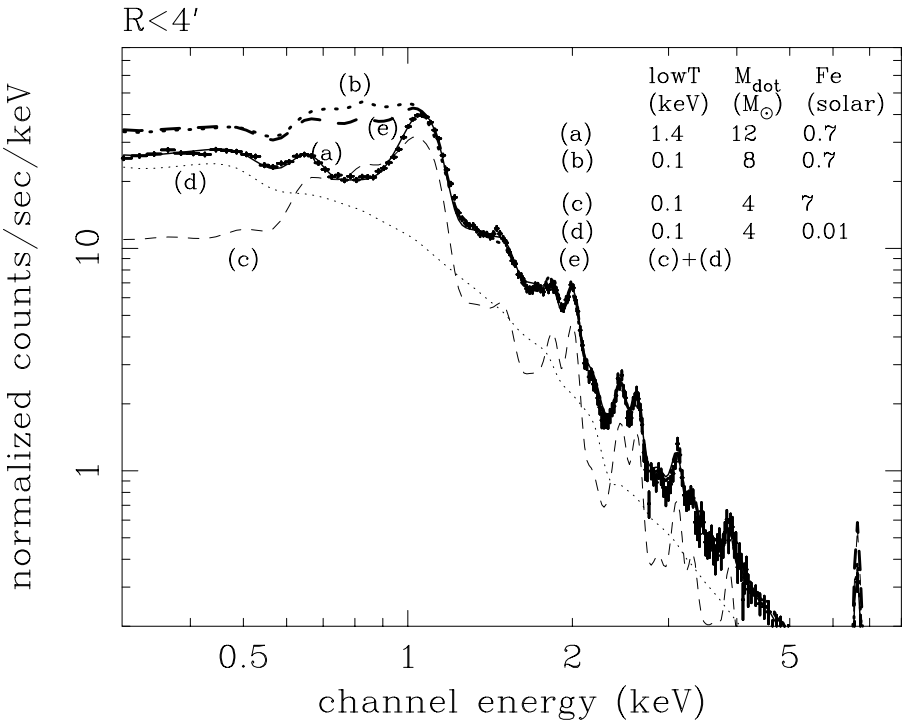

Figure 2: Deprojected spectra within $R < 4'$ fitted with a cooling flow model with a cut-off temperature, lowT=1.44 keV (solid line, a). The bold dotted line show the model which cool down to 0.1 keV (bold dotted line, b). The thin dashed line and the dotted line corresponds to the model with a model with 10 times higher metallicity and a model with low metal abundance, respectively. The bold dahsed line is the sum of the high and low abundance models.

$R > 0.5'$, the ICM at a given radius is dominated by only a single temperature component. There is a small amount of a cooler component with a temperature of 1 keV, mainly linked to the radio libes region. Moreover, temperature obtained from MEKAL model seems to be reasonable at least in the obtained temperature range.

1.3 Application of the cooling flow model

At $R = 4'$, the derived cooling time is only a few Gyr and $\dot{M}_{\rm I}$ is 8 $M_{\odot}{\rm y}^{-1}$, respectively. The net effect of resonance scattering is negligble for the radiative output in this integrated circular region. Without any heating, the gas should cool down to 0 keV, emitting X-rays. Therefore, the spectral cooling rate, $\dot{M}_{\rm S}$, within the radius should be $8M_{\odot}{\rm y}^{-1}$.

We fitted the deprojected spectra within $R < 4'$ with a cooling flow model using the MEKAL code modified by photoelectric absorption. As in other cooling flow clusters observed by RGS, in order to fit the spectra, we need a cut-off temperature, lowT, which is found to be 1.4 keV. Figure 2 shows the EPN spectra within $R < 4'$, fitted with the cooling flow model. We also plotted in the figure, other cooling flow model with lowT to 0.1 keV, fitted only to the data in the spectral range above 1.2 keV. The difference in the continuum level between 0.2 and 0.5 keV is due to the instrumental low-energy tail of Fe-L and O-K lines. The component cooling radiatively to 0 keV should emit strong Fe-L lines between 0.6 to 1.0 keV, which are not seen in the spectrum.

When adding a isothermal MEKAL component, we can fit the spectra with a cooling flow component with lowT=0.1 keV. However, $\dot{M}_{\rm S}$ is only 0.8 $M_{\odot}{\rm y}^{-1}$, which is a factor of 10 smaller than $\dot{M}_{\rm I}$ at the same radius.

Fabian et al. (2001) made a proposal to solve the cooling flow problem, that metals in ICM

are not uniformely distributed. In this suggestion, a metal poor part of the gas cools without emitting lines and a metal rich part cools rapidly. In this way, total strength of Fe-L line emission should be reduced. Figure 2 also shows an example of a bimodal metal model which is sum of a metal poor and a metal rich component. Because of the dependence of the cooling function on metallicity, the total Fe-L spectrum depends on the metallicity distribution. The metal rich component also emit strong Fe-L lines below 0.9 keV, alghough its strength is slightly reduced, but the combined effect is small. Therefore, any multi-abundance model cannot explain the observed Fe-L profiles. In order to explain it, we needs a sharp cut off in the temperature distribution.

2 Discussion

The standard cooling flow model indicate that the ICM is multi-temperature on small scales, since mass is thought to be deposited within the whole cooling flow region. The cooling matter should emit strong Fe-L lines below 0.9 keV. We cannot detect a spectral cooling flow component from the whole field of view of the detector and the ICM at any given radius is dominated by a single temperature component. The upper limit of $\dot{M}_{\rm S}$ is an order of magnitude smaller than $\dot{M}_{\rm I}$. A bimodal metal abundance distribution model cannot explain the observed Fe-L profile.

The resonance scattering may reduce the strength of some resonance lines. However, all the Fe-L lines below 0.9 keV, which includes both resonance lines and non-resonance lines, are suppressed from the expected value. In addition, the spectral cooling flow component is also small where the resonance scattering is not effective. Therefore, the resonance scattering is not the cause to suppress the Fe-L lines below 0.9 keV.

At 1 r_e of M 87, $\dot{M}_{\rm I}$ is $\sim 4 M_\odot yr^{-1}$. In contrast, the upper limit of $\dot{M}_{\rm S}$ is $\sim 0.4 M_\odot yr^{-1}$. This value is close to the stellar mass loss rate within 1 r_e, which is 0.5 $M_\odot yr^{-1}$. At this radius, $t_{\rm cool}$ is 10^9yr and gas mass is $210^9 M_\odot$. In addition, there is a strong Fe and Si gradient around M 87 (Böhringer et al. 2001). The scale of the gradient, which is only several kpc, and the abundance ratio indicates that the gradient is mainly caused by SN Ia in M 87. The Fe and Si abundances of normal X-ray luminous galaxies such as NGC 4636 are about 1 soloar (e.g. Matsushita et al. 1997; 2000). The standard cooling flow model indicates that the cooling flow rate of these galaxies are $\sim 1 M_\odot yr^{-1}$. If a cooling flow with mass deposition rate of $\sim 4 M_\odot yr^{-1}$ exists, the abundance gradient must be reduced compared to the observed value. The fact indicates that the ICM within 1 r_e is dominated by gas ejected from M 87. Therefore, the overall cooling flow expected from the classical galaxy cluster cooling flow model, should not exist in M 87, although a small scale cooling flow, with mass deposition rate close to the stellar mass loss rate, may exists in the central core of the classical cooling flow regions.

References

1. E. Belsole *et al*, A&A **365**, 188 (2001).
2. H. Böhringer *et al*, MNRAS **274**, 67 (1995).
3. H. Böhringer *et al*, A&A **365**, 181 (2001).
4. A.C. Fabian *et al*, ApJ **248**, 47 (1981).
5. A.C. Fabian, ARA&A **32**, 277 (1994).
6. A.C. Fabian *et al*, MNRAS **321**, 20 (2001).
7. E.D. Feigelson *et al*, ApJ **312**, 101 (1987).
8. P.E.J. Nulsen and H. Böhringer, MNRAS **274**, 1093 (1995).
9. K. Matsushita *et al*, ApJ **488**, 125 (1997).
10. K. Matsushita *et al*, PASJ **52**, 685 (2000).
11. G.C. Stewart *et al*, ApJ **278**, 536 (1984).